Indian Journal of Geo-Marine Sciences
Vol. 39(4), December 2010, pp. 475-484

Variability of coastal ocean processes along the west coast of India

A. D. Rao

Centre for Atmospheric Sciences, Indian Institute of Technology Delhi, Hauz Khas, New Delhi 110 016, India
[E-mail: adrao@cas.iitd.ernet.in]

Received 20 August 2010, revised 21 December 2010

Three-dimensional Princeton Ocean Model (POM) is used to understand coastal ocean processes and its variability along the west coast of India. An attempt is first made to understand variability of the surface circulation and associated SST during July-August 2000 and 2002 as a response of daily wind stress forcing derived from the QSCAT winds. The coastal current reverses its direction to either off-shore or northward if the wind reduces its strength suddenly to less than 3 ms^{-1} towards the coast. In this event, the coastal upwelling is inhibited by the reversal of near shore currents and results in an increase in the local SST. This feature is also noticed in the buoy data available for 2002. Another experiment is made to understand the dynamics in relation to the fact of observed low-salinity plume off Gulf of Khambhat during post-monsoon season. It is found that the freshwater discharge to the gulf from the adjoining rivers during monsoon season is trapped in the region as the currents are onshore. As the currents change its direction to offshore after withdrawal of the monsoon, the confined low-salinity waters are being released to the open ocean. Lastly, the study is made to understand the response of the ocean to tropical cyclones in the Arabian Sea (AS). The study focuses on surface cooling and temperature rise in the sub-surface waters and explained its mechanism through upwelling and downwelling processes respectively. Local stratification of the vertical temperature plays an important role for the cooling of the surface waters and warming in the sub-surface depths. The analysis of the model simulations and observations suggest that the extent of sub-surface warming is directly related to the depth of the thermocline region.

[**Keywords:** Arabian Sea, Coastal circulation, Numerical modeling, Tropical cyclone, Subsurface warming]

Introduction

Luis and Kawamura[1] studied the upwelling processes near the southern tip of India as a result of gap wind event (blowing in the Palk Strait) during pre-monsoon season. The gap winds are generally low-level strong winds of 20-40 knots blowing through a gap between mountains. Luis and Kawamura[2] noticed that during SW monsoon the surface cooling due to coastal upwelling promoted by the alongshore wind stress overwhelms the surface heat loss. The coastal upwelling along the west coast of India is recently studied[3,4] during pre-monsoon and monsoon seasons using POM. As the coastal upwelling process is a transient phenomenon, an attempt is made in the present paper to capture variability of shelf circulation and associated coastal upwelling processes in the South-Eastern Arabian Sea (SEAS) as a response of wind alone on the temporal and spatial scales.

Even though there are no major river systems along the west coast of India compared to the east coast, it is interesting to study the effect of freshwater discharge on the coastal circulation. The Indus, Mahi, Narmada and Tapti are the main rivers which discharge freshwater into the eastern Arabian Sea (AS). The freshwater outflow from the Indus River inhibits the upwelling tendency of the isotherms in the surface layer[5-7]. Shankar *et al*.[8] studied the water-masses off the southeastern Arabian Sea during 2002 summer monsoon. Their study suggests that the freshwater discharge from various rivers located along the west coast of India and rainfall over the Western Ghats forms a layer of low-saline waters over the eastern AS that has a short-life cycle. The present study is focused to the region of Gulf of Khambhat. The paradoxical nature of the observed salinity field in the waters of this region is pointed out here. The low-salinity plumes are observed in the post-monsoon season and not during the monsoon as may be expected. This has been explained by the local circulation of the region through model studies using the POM. Though the model has been implemented for the entire eastern part of the AS, the simulations are focused particularly for the northeastern region near the gulf. In the present study, the rivers namely Indus, Narmada, Tapi and Mahi are incorporated in the model by replacing rigid boundary condition by an open-boundary at the coast where these rivers are joining the AS.

There are only few modeling studies of cyclones in the eastern AS. Bender and Ginis[9]; Mahapatra *et al.*[10]

studied using the POM the ocean's response due to passage of any cyclone mostly related to surface ocean cooling. However, Zedler *et al.*[11] studied the upper ocean response to hurricane Felix and observed the associated cooling in the upper 30m and warming at depths of 30-70m. They simulated the temperature evolution during cyclone period with one-dimensional mixed layer model. Here, the response of the eastern AS to a tropical cyclone is studied using the POM. Two recent past cyclones during June 1998 and May 1999 that crossed northern west coast of India are chosen. The study is confined to the simulations of temperature and currents during and after the passage of the cyclone to understand the mechanism of surface cooling and the subsurface warming on either side of the cyclone track.

Materials and Methods

Data

The tracks of 1998 and 1999 cyclone from the Unisys Weather Information Services are shown in the Fig.1. The numbers on the track gives the dates corresponding to different location at 0600 UT. These cyclones are having almost the same intensity of 40 ms^{-1} at the time of crossing DS1 location. Real-time measurements of marine meteorological and oceanographic parameters were acquired at DS1 (Deep Sea) buoy location (15.5° N, 69.2° E) in the AS (Fig.1), where the local depth is about 3500m. The meteorological parameters such as air pressure and winds are measured at 3m above the sea surface while; surface currents and SST are observed at 2.5m below the sea surface. Apart from these parameters, one of the critical parameter i.e. water temperature at different depths is available only for June 1998 cyclone. This was measured using thermistor chain fitted along with the mooring rope upto 100m depth. These observations provide an opportunity to understand the variation of temperature and current due to passage of the cyclone. Fig. 2 depicts the observed time series temperature when the June 1998 cyclone was passing near to DS1 location. The

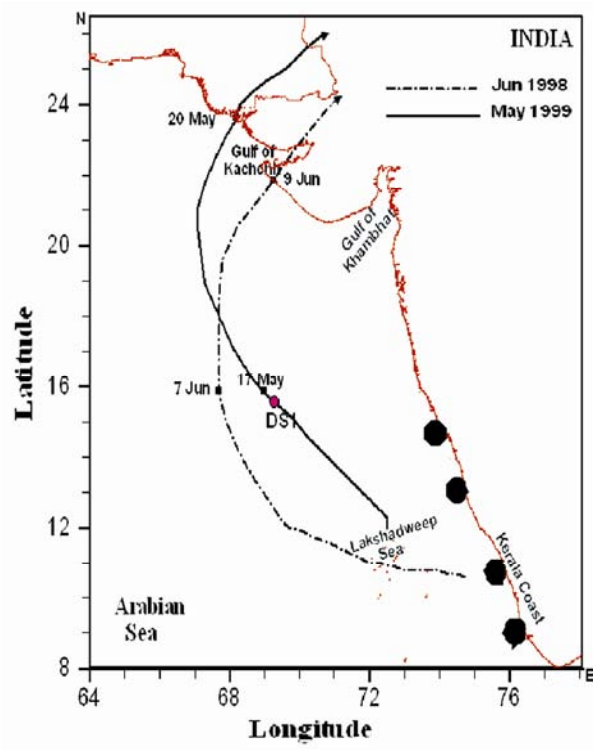

Fig. 1—Analysis area with cyclone tracks.

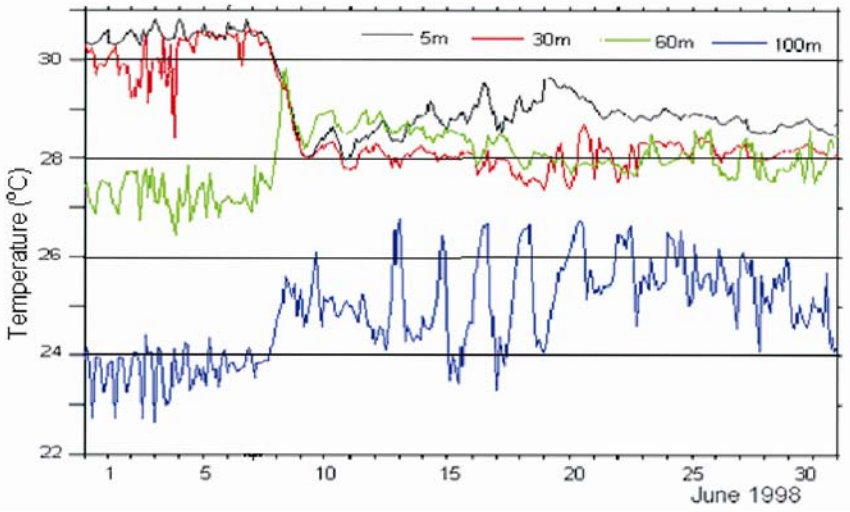

Fig. 2—Observed time series of temperature at different depths for June 1998 cyclone at DS1 location.

analysis of the data suggests that cooling in the surface layers is noticed upto 30 m and warming beneath 30 m to 100 m depth. The periodicity of the inertial oscillations at any latitude is given by $\frac{2z}{f}$ where f is the earth's angular speed at given latitude. Accordingly, strong inertial oscillations of periodicity of about 2 days are generated at 15.5°N by the cyclone in the subsurface layers. In the present paper, our concern is mainly on understanding the possible mechanism of subsurface warming due to the passage of cyclone. To understand this phenomenon, model results are first analyzed and compared with the available *in-situ* observations.

The monthly climatological freshwater discharge of the various rivers in the northeastern AS is obtained from global river discharge database (http://www.sage.wisc.edu/riverdata/). Monthly discharge for these rivers is given in Table 1. The freshwater outflow varies seasonally with its maximum during June to August (monsoon). The maximum discharge is seen from the Indus River followed by Narmada, Tapi and Mahi that are located in the gulf region. The monthly climatological salinity of WOA05[12] is depicted for Jul, Oct and Dec in Fig 3 (a-c). Locations of the rivers Narmada, Mahi, Tapi and Ozat are shown in the figure by the numbers 1, 2, 3 and 4 respectively. However, the location of the Indus River (24° N, 67.5° E) is just outside the analysis area. Low-salinity water of 34 psu is noticed in October in the region close to the gulf compared to that of other months. Using the ARGO data, the salinity variation (averaged for the 17-20°N) is shown in Fig 3(d) for 2004. The data is obtained from INCOIS web site

Table 1—Fresh-water River Discharge (m^3s^{-1}) from Global River Discharge Database from http://www.sage.wisc.edu/riverdata/index.php?qual=32

River name	Jan	Feb	Mar	Apr	May	Jun	Jul	Aug	Sep	Oct	Nov	Dec
Indus	647	1027	1000	1431	2279	3999	6361	6875	3405	1520	1112	725
Narmada	116	85	61	44	29	294	1835	4336	4074	934	237	190
Mahi	13	11	24	9	6	158	659	1528	1652	93	30	19
Tapi	39	35	38	37	31	119	415	844	847	145	48	52
Ozat	0	0	2	0	0	0	16	10	5	1	0	0

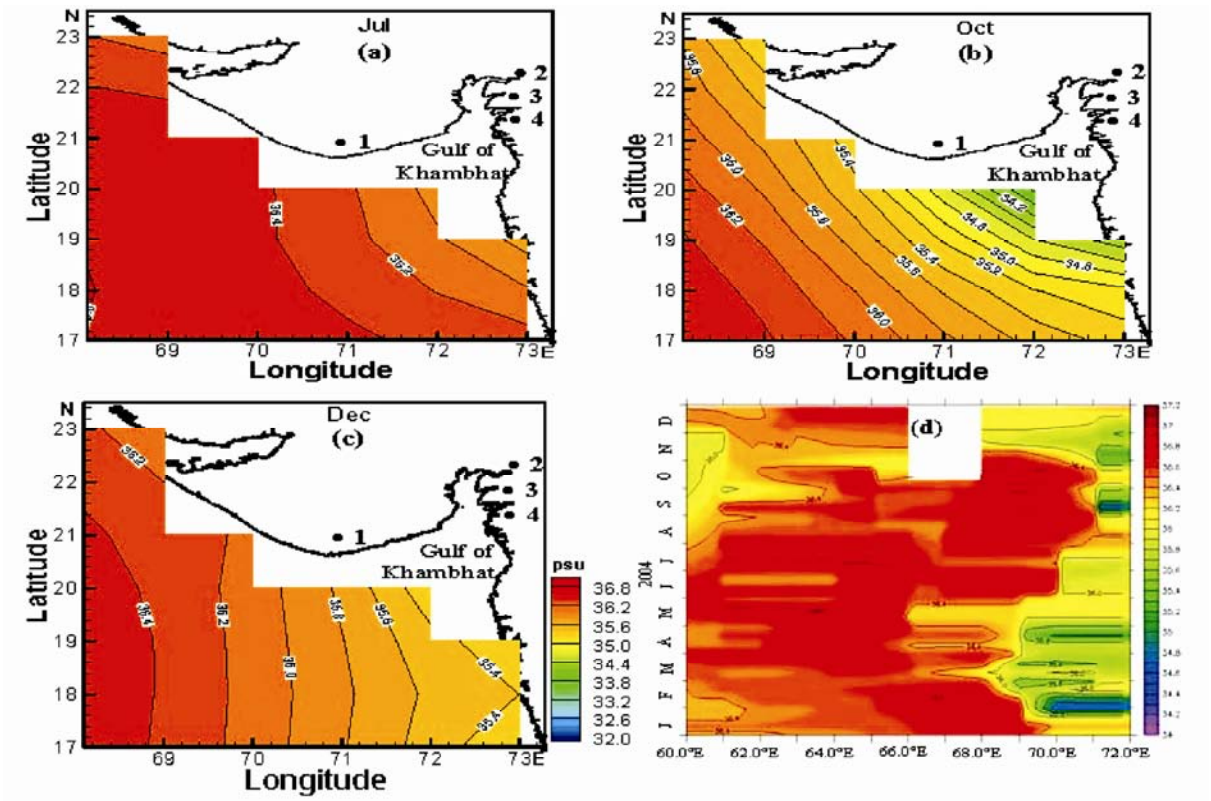

Fig. 3—Monthly climatological salinity for (a) July, (b) October (c) December (d) ARGO observations averaged for 17-20N during 2004

http://www.incois.gov.in/. Low-salinity plumes in the region during post-monsoon months are clearly seen. Fig 4 shows an area-averaged time-series of surface salinity from ARGO data over a box of 3 deg (17-20N, 69-72E) for the years 2004-06 and monthly climatology of salinity. Low-salinity plumes in the region during post-monsoon months are clearly seen in all the years with large inter-annual variability. The existence of low-salinity waters off Gulf of Khambhat region during post-monsoon season has warranted in studying the origin of these waters, which extends even up to December.

Numerical Experiments

The POM model is implemented for the eastern AS. The model used here is same as that used in Rao *et al.*[4], for the study of coastal upwelling along the west coast of India in which model setup and description are given comprehensively and hence the details are only given here in brief. The analysis area approximately extends from 4°N to 24.5°N along the eastern AS with an offshore extent of ~600 km parallel to the coast (Fig 1). Resolution in zonal direction varies from 6-9 km with finer resolution near the coast whilst, it is ~10 km in meridional direction with 175×250×26 computational grid points. The model grid size near the coast resolves internal Rossby radius of deformation which varies from10-50 km. The model uses mode splitting technique. The two dimensional external mode uses a short time-step of 11.25 sec based on the Courant-Freidrch-Levy condition and the external wave speed, while, three-dimensional internal mode uses a long time-step of 480 sec based on the internal wave speed. Along the open-boundaries, radiation type of conditions are used to allow disturbances generated from the interior to travel outwards as progressive waves[3,7]. For temperature and salinity, upstream advection scheme is applied. Initial data fields of temperature and salinity are obtained from World Ocean Atlas 2001[13]. The model surface forcing is derived from the daily QuickSCAT winds of 0.25° horizontal resolution. In this study, the surface fluxes are not considered as the prime objective is to study only the affect of the wind on the shelf circulation. Four stations A, B, C, D are selected along the coast as shown in Fig 1 in order to study the circulation at different latitudes. The buoy observations of SW4 which is located near to the station C is used for validation of the model simulations.

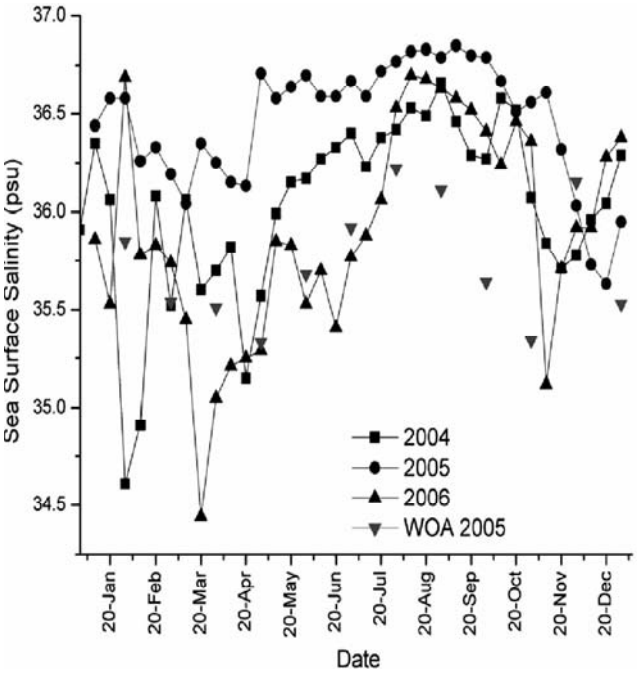

Fig. 4—Time series plot of surface salinity averaged over a box of 3×3 degrees.

Results and Discussion

(a) Response of winds on shelf circulation

To study the variability in shelf circulation and associated thermal response during July-August for the years 2000 and 2002, two experiments have been carried out keeping the same initial conditions for temperature and salinity. The model is forced with the corresponding wind stress after interpolating at the model grid points. Initially, the model is integrated in the diagnostic mode for 25 days until the kinetic energy of the system achieves nearly a steady state[14]. The model integration is then carried out further for 50 days starting from 21 June and results are analyzed from 1 July focusing along the Kerala coast.

To investigate further, the cause of reversal of coastal currents in the month of July and August, time variation of QSCAT wind speed (used in the study) and associated simulated surface current is plotted for 2000 and 2002 in Fig 5 and 6 respectively at the locations of A, B, C, D. As shown in Fig 1, stations A and B are located north of Kerala; stations C and D are located along the Kerala Coast. If the current direction is between 140° - 220°, the flow direction is then considered as southward and if the direction is between 270° -360° or 0°- 45°, it is northward. The variation in wind magnitude is noticed along all the points with maximum range at C and D locations. It is evident from the figures that flow pattern at A and B is southward throughout the period but its direction

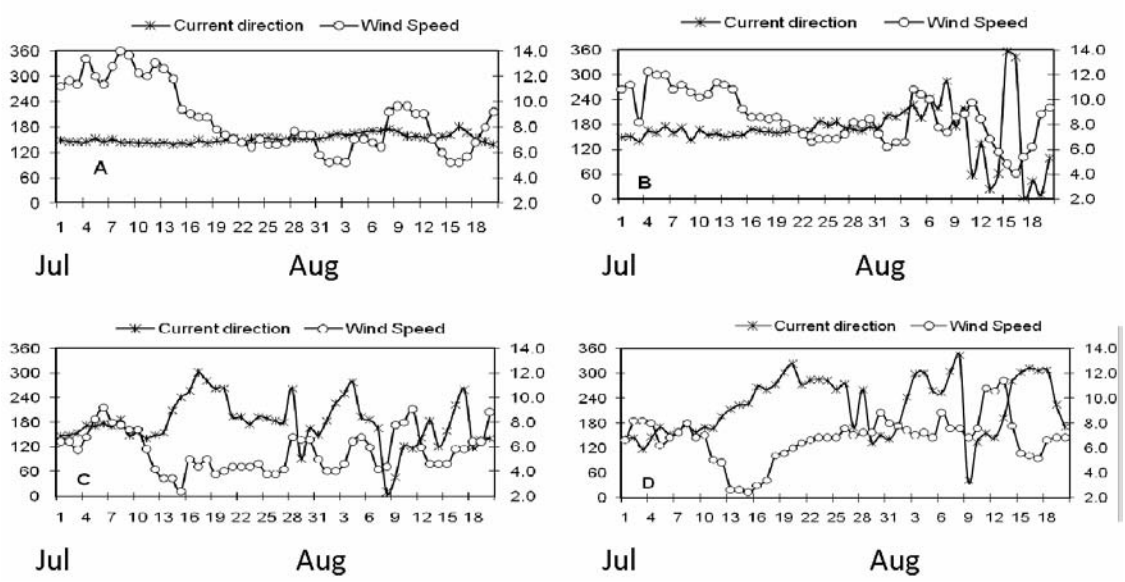

Fig. 5—Wind speed (ms^{-1}) and direction of surface current (deg) for 2000.

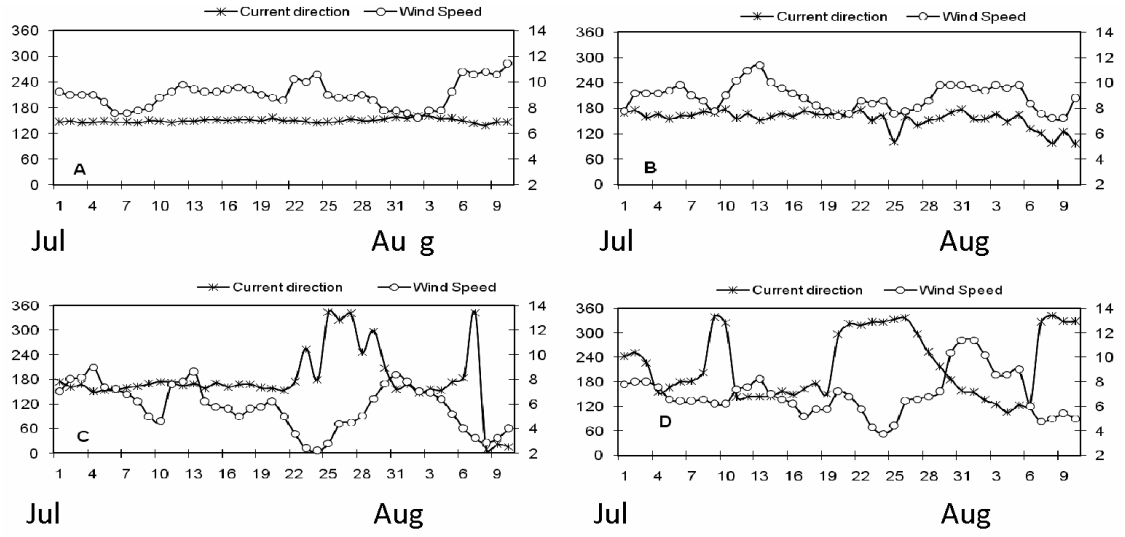

Fig. 6—Wind speed (ms^{-1}) and direction of surface current (deg) for 2002.

varies at C and D. It is noticed whenever the wind speed near the coast (within 50km from the coast) decreases (< $3ms^{-1}$) there is formation of reversal in the current direction in the region. Strength of the reversed current is also inversely proportional to strength of the wind near the coast. It is also observed that there is 1-2 days lag between the reduction in winds and the reversal of currents.

To verify further existence of reversal currents near the coast, time variation of SW4 buoy wind speed and current direction for July-Aug 2002 are depicted in Fig 7. To avoid the land and sea breeze effect, the early evening to late morning data observation has been removed. That means the observations between 9am-4pm are considered here to get the daily variations from the buoy data. It is observed from the buoy data, the currents are reversed when the winds fell below $3ms^{-1}$ near the coast. It means that whenever there is a decrease in the wind speed, the current direction becomes northward. It is found that the correlation coefficient is 0.8 between model simulated and observed currents for 2002. Hence, the model simulations described above are consistent with the feature noticed in the observations. The time

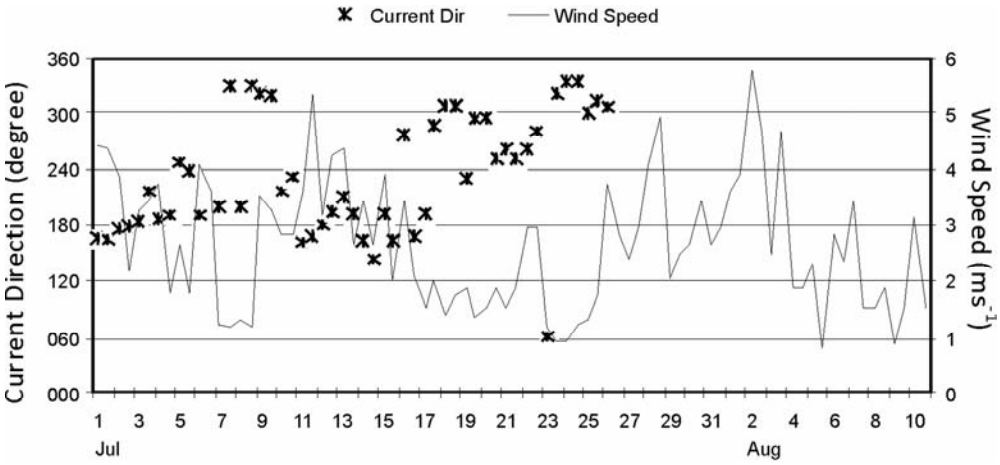

Fig. 7—SW4 Buoy wind speed and current direction Jul-Aug 2002.

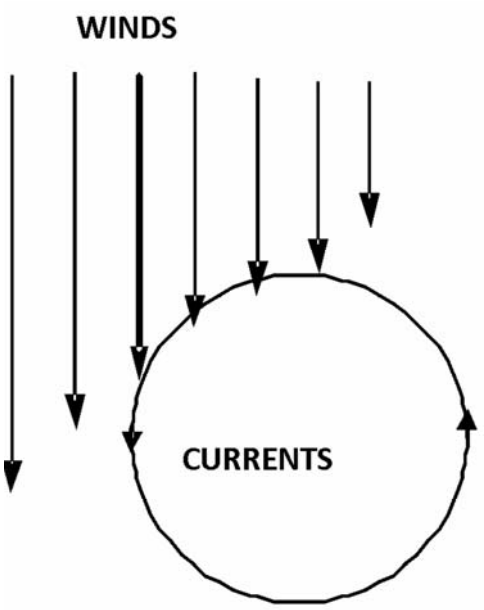

Fig. 8—Schematic of local vorticity due to zonal variation in wind magnitude.

lag between the reduction of winds and reversal of currents is also seen in the observations.

It is also important to understand the possible mechanism for reversal of coastal currents in the event of any decrease of wind strength towards the coast. To make this point more apparent, a schematic diagram is shown in Fig 8 depicting a cyclonic eddy formed as result of zonal wind variation. As it understands from the figure, the distribution of wind field when its magnitude decreases towards the coast it would help to form a local anti-clockwise vorticity in the ocean. As the winds modulate on synoptic scale, the vorticity would play an important role on the local costal dynamics. Hence, it may be concluded that the weak winds prevailing off Kerala coast is the main cause for the reversal of the coastal currents.

(b) Impact of freshwater discharge in the Gulf of Khambhat

To investigate the origin of low-salinity plumes during post-monsoon season, the model is integrated from July to December. The simulated surface circulation is shown in Fig 9 only for July, October and December. During July, the shelf is dominated by strong southwesterly winds (10-15ms^{-1}), leading to strong southerly current all along the coast except in the region off Gulf of Khambhat. The model simulates the strength of the WICC about 35-45 cms^{-1}, whereas the currents in the gulf region are very weak. In the transition period (September - October), the West India Coastal Current (WICC) is weak and variable. With the arrival of winter in November, the northeasterly winds reduce their strength significantly (~2-5ms^{-1}) and continues during this season. During December, the simulated WICC is northward along the coast, except the region near Gulf of Khambhat. It is very important to note that the simulated currents are southerly off the Gulf region.

From the simulated current pattern and prevailing salinity distribution, it suggests that the currents in the Gulf region during summer monsoon are onshore that prevents low-saline waters to advect offshore as the rivers discharge freshwater in the region. In the transition period, the prevailing currents slowly turn into offshore and continue till winter. These offshore currents would help in flushing-out the low-saline waters during this season that were trapped during monsoon period as the currents were not favorable. The simulated currents off the west coast of India are,

in general, in good agreement with the mean monthly current vectors derived from satellite tracked drifting buoys data over 2° square[15]. However, there are no in-situ or buoy current observations available close to the gulf region for comparison of simulations in this region.

The Temperature Inversions (TI) are known to occur during winter in the near surface ocean regime where salinity stratification is large enough to influence the density field[16]. In the region of Gulf of Khambhat, the low-saline waters during winter provide stable salinity stratification. The stratification along with the winter time cooling would enhance the prospects of formation of TI in this region. This has been confirmed from available ARGO data north of 17°N. Fig 10 shows vertical temperature (full-line with symbol) and salinity (full-line) profiles. The legend inside the each box gives the profile ID given by WMO (first row), location (second row) and date (third row). The TI can be clearly noticed upto 19°N during December-February and its range varies from 0.2-1.0°C. It is important to mention that the TI in the northern latitudes can be seen even up to the depth 75 m and this depth also coincide with the depth where Arabian Sea high salinity water exists with the surface layer having low-salinity waters advected from the gulf region.

(c) Response of sub-surface waters in the eastern AS to Tropical Cyclones

Initial temperature and salinity fields are obtained from World Ocean Atlas 2001. Thermal forcing is

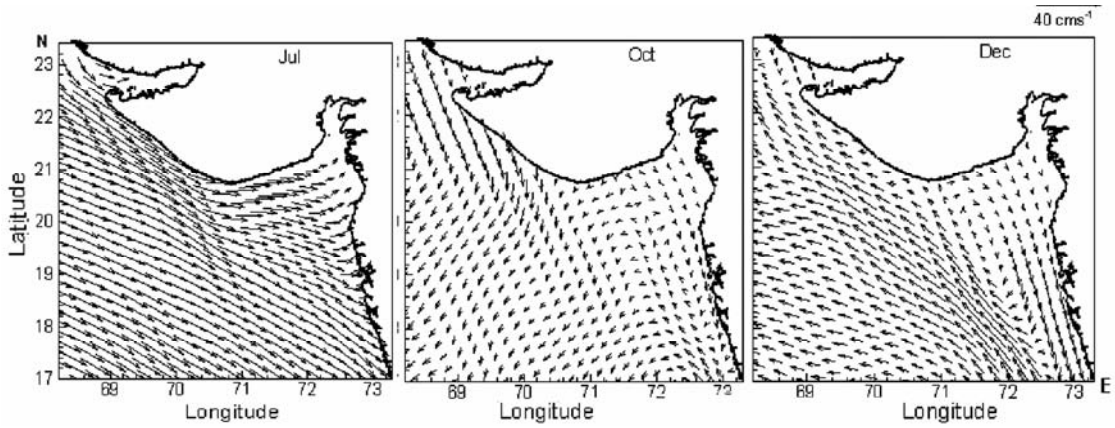

Fig. 9—Simulated surface currents (cms^{-1}).

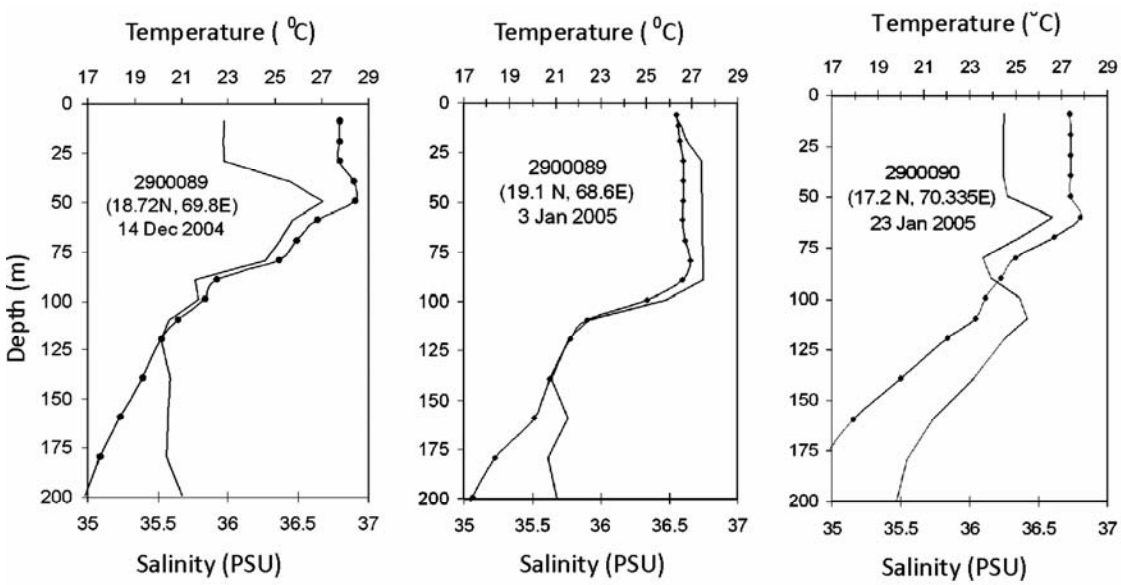

Fig. 10—ARGO ~~obser~~vations of salinity (◆—◆) and temperature ( ) during winter.

used from Lisan and Weller[17] heat flux data at $1^{o}\times1^{o}$ in terms of daily incoming solar radiation and the net heat flux. The wind stress at the model surface is derived from ECMWF winds (2.5°×2.5° gridded data). With these initial data fields, the model integration is started about 15 days before the cyclone forms over the ocean. It is to be noted that neither ECMWF nor high resolution scatterometer winds are able to capture the high intensity of the cyclone. Hence, wind field for both cyclones have been generated using the asymmetric wind module of Jelesnianski and Taylor[18]. Comparison of model wind speed with that of observed at DS1 location is depicted in Fig.11 for both the cyclonic events. In the case of 1998 cyclone, maximum wind speed observed is of ~ 25ms^{-1} (Fig.11a) on 7 June when the cyclone is nearest to the buoy position. The computed cyclonic winds at the DS1 location are comparable with buoy observations. Since, the wind speed becomes normal after 9 June, the model is again forced with the ECMWF daily winds in the absence of QuikSCAT winds during this period. The model net heat flux during this period is also depicted in the figure along the secondary axis in which positive values indicate the gain and negative corresponds to the loss with reference to the ocean. The net heat flux is negative during the cyclone period 6-9 June and then positive till 18 June. Later, the flux decreases again as onset of the monsoon winds strengthen. Similar comparison is also noticed for May 1999 cyclone as depicted in Fig.11b.

The daily SST of the model and DS1 buoy for the 1998 and 1999 cyclones are depicted in Fig.12 at the location of DS1. It is noted for 1998 cyclone (Fig.12a) that there is a sudden drop in SST immediately following the passage of the cyclone. There is a sharp fall of SST of about 2.5°C within 24 hours after crossing the cyclone at DS1 on 7th as the net heat flux reduces significantly. The maximum cooling due to the passage of the cyclone is in agreement with the buoy value. After 8th, the SST returns slowly to normal variations, but colder temperatures than before the storm. As the southwest monsoon picks up its strength after 19th, the winds are strong and hence causing more evaporation. As a result, the sea surface cooled, as is evident from the fluxes that are negative during this period (Fig 11a). The simulations for the 1999 cyclone also suggest similar pattern as shown in Fig 12. However, the associated cooling is only about 1.5°C which is about 1°C less compared to 1998 cyclone.

In order to understand the thermal response across the depth at DS1, the computed temperature at different depths is plotted in Fig.13 for the cyclones. In either case, the temperature at 5m depth shows a sharp decrease immediately after the cyclone passes the location. It is found that the surface waters are cooled by more than 2.5°C in the case of 1998 cyclone (Fig. 13a). An increase of temperature of about 1.7°C at

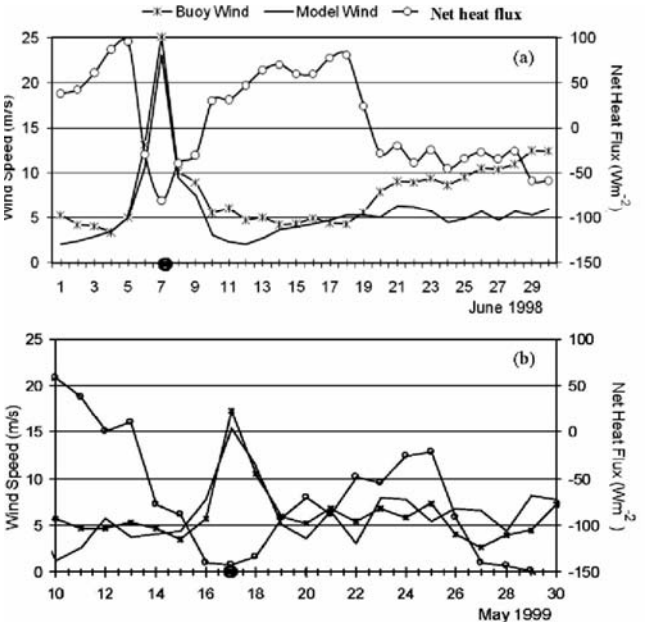

Fig. 11—Model and buoy wind speed along with surface net heat flux at DS1 location for 1998 and 1999 cyclone events.

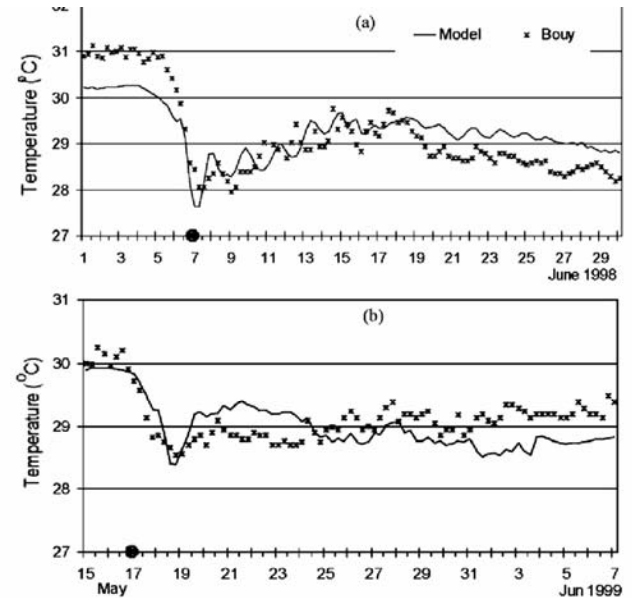

Fig. 12—Comparison of model SST with buoy data at DS1 location for 1998 and 1999 cyclone events.

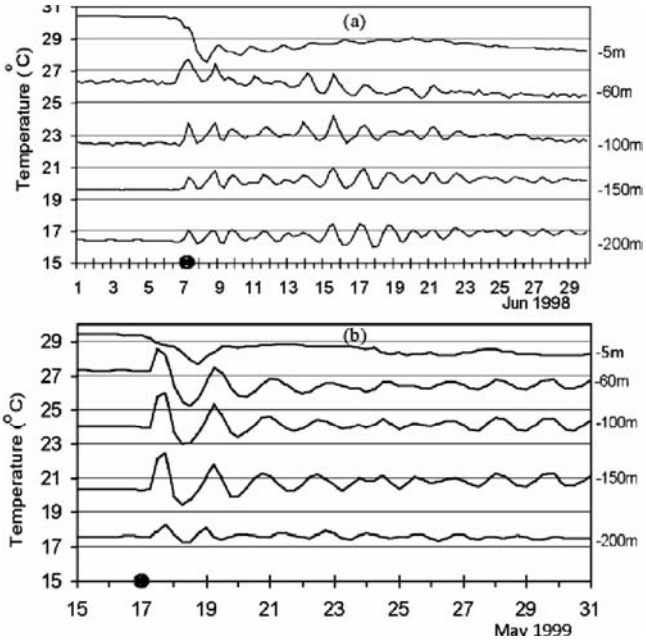

Fig. 13—Time variation of model temperature at different depths for 1998 and 1999 cyclone events.

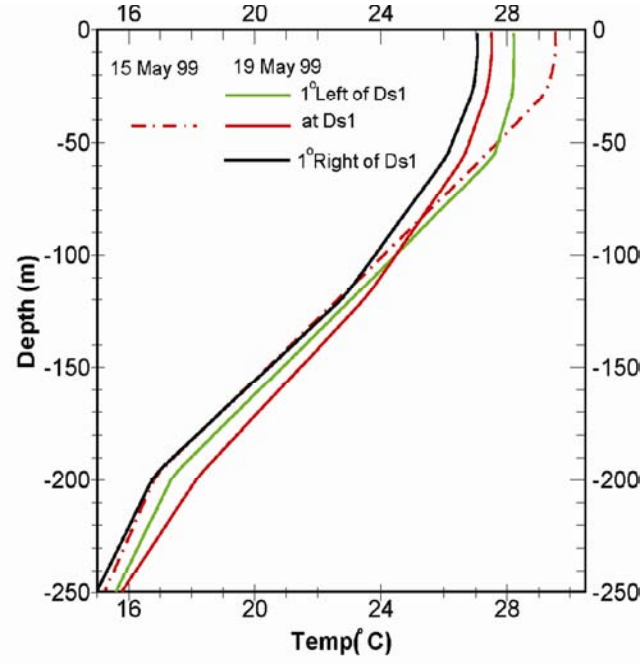

Fig. 14—Vertical temperature profile at locations to the left, right and centre of the cyclone.

60m is simulated and the magnitude of the increase reduces with the depths below. Though the increase is underestimated compared with the observations, the model is still able to simulate reasonably well. In general, the depth at which an increase of sub-surface temperature depends on the local thermocline depth. The temperature decreases at 60m depth after 15 June may be related to the surface cooling as the monsoon winds become stronger which is also noticed. The inertial oscillations generated by the cyclone are continued for about two weeks. These simulations are consistent with the observations (Fig 2). In the case of 1999 cyclone (Fig. 13b), the surface cooling of only 1°C is simulated as it may be because of the buoy location coincides with the centre of the cyclone. However, in the subsurface depths of 60-200 m, a sudden rise of temperature is computed as soon as the cyclone crosses the location. The associated subsurface warming of about 2°C is noticed below the depths of 60 m.

The centre of the 1999 cyclone coincides with the buoy location. Hence, it is interesting to see how the surface water is cooled on either side of the DS1. Fig 14 provides the computed thermal profiles for 1999 cyclone at selected locations through depth before and during the cyclone crossing the DS1 location. The locations are selected about one degree left side and right side to the buoy location when the cyclone was crossing on 19 May. These profiles are compared with the initial temperature profile before the cyclone period on 15 May. The warming of sub-surface waters occurs only on the left side of the track as a result of downwelling in the region. The surface cooling is more than 1°C on the right side of the track compared to that of left due to strong upwelling in addition to evaporative cooling on either side.

References

1 Luis, A.J. & Kawamura, H., A case study of SST cooling dynamics near the Indian tip during May 1997, *J. Geophys. Res*., 107(C10)(2002) 11, doi: 10.1029/2000JC000778.

2 Luis, A.J. & Kawamura, H., Seasonal SST patterns along the West India shelf inferred from AVHRR, *Remote Sensing of Environment*, 86(2003) 206–215.

3 Rao, A.D. & Joshi, Madhu., Modelling of Upwelling Processes during Pre-Monsoon and Monsoon along the West Coast of India, *International Journal of Ecology and Development*, 10(2008) NS08.

4 Rao, A.D., Joshi, Madhu. & Ravichandran, M., Oceanic upwelling and downwelling processes in waters off the west coast of India, *Ocean Dynamics,* 58(3-4)(2008) 213-226, doi: 10.1007/s10236-008-0147-4.

5 Sanilkumar K V & Unny V K, *Upwelling characteristics off the Saurashtra coast during 2004*, (Proceedings of National workshop on Oceanographic features of Indian coastal waters) 2005, pp. 113-118.

6 Rao, A.D., Joshi, Madhu. & Babu, S.V., A three dimensional numerical model of coastal upwelling along the west coast of India, *Mathematical and Computer Modelling*, 41(1-2) (2005) 177-195.

7 Rao, A.D., Joshi, Madhu. & Ravichandran, M., Observed low-salinity plume off Gulf of Khambhat, India, during

post-monsoon period, *Geophy. Res. Lett*., 36(2009) 1-4, doi: 10.1029/2008GL036091.

8 Shankar, D., Shenoi, S.S.C., Nayak, R.K., Vinayachandran, P.N., Nampoothiri, G.S., Almeida, A.M., Michael, G.S., Ramesh Kumar, M.R., Sundar, D. & Sreejith, O.P., Hydrography of the eastern Arabian Sea during summer monsoon 2002, *J. Earth Syst. Sci.*, 114(2005) 475-491.

9 Bender, M.A. & Ginis, I., Real case simulations of Hurricane-Ocean Interaction Using a High-Resolution Coupled Model: Effects on Hurricane Intensity, *Monthly Weather Review*, 128(2000) 917-946.

10 Mahaptra, D.K., Rao, A.D., Babu, S.V. & Chamarthi Srinivas., Influence of Coastline on Upper Oceans Response to the tropical cyclone, *Geophy. Res. Lett*., 34(2007) 1-3, doi:10.1029/2007GL030410.

11 Zedler, S.E., Dickey, T.D., Doney, S.C., Price, J.F., Yu, X. & Mellor, G.L., Analyses and simulations of the upper ocean's response to Hurricane Felix at the Bermuda Testbed Mooring site: 13–23 August 1995, *J. Geophys. Res.*, 107(C12) (2002) 3232, doi:10.1029/2001JC000969.

12 Boyer, T., Levitus, S., Garcia, H., Locarnini, R., Stephens, C. & Antonov, J., Objective Analyses of Annual, Seasonal, and Monthly Temperature and Salinity for the World Ocean on a ¼ degree Grid, *Journal of Climatology,* 25(2005) 931-945.

13 Conkright M E & Boyer T P, *World Ocean Atlas 2001: Objective Analyses, Data Statistics, and Figures*, (CD-ROM Documentation, *National Oceanographic Data Center, Silver Spring 2001*, MD) 2002, pp. 17.

14 Ezer, T. & Mellor, G.L., Diagnostic and prognostic calculations of the North Atlantic circulation and sea level using a sigma coordinate ocean model, *J. Geophys. Res.,* 99(C7)(1994) 14159-14171, doi: 10.1029/94JC00859.

15 Rao L V G & Shree Ram P, *Upper ocean physical processes in the tropical Indian Ocean*, (A monograph prepared under CSIR emeritus scientist scheme, National Institute of Oceanography, Goa) 2005, pp. 1- 492.

16 Durand, F., Shetye, S.R., Vialard, J., Shankar, D., Shenoi, S.S.C., Ethe, C. & Madec, G., Impact of temperature inversions on SST evolution in the southeastern Arabian Sea during the pre-summer monsoon season, *Geophys. Res. Lett.,* 31(L01305)(2004) 4, doi: 10.1029/2003GL018906.

17 Lisan, Y. & Weller, R.A., Objectively Analyzed Air-Sea Heat Fluxes for the Global Ice-Free Ocean (1981-2005), *Bulletin of the American Met. Society*, 88(2007) 527-537.

18 Jelesnianski C P & Taylor A D, *A preliminary view of storm surge equations of motion with amildly curved coast,* (NOAA Technical Memorandum*,* ERL 1973, WMPO-3) 1973, pp. 23-33.